RSC Advances

PAPER

View Article Online
View Journal | View Issue

Cite this: *RSC Adv.*, 2022, **12**, 19445

Chemical constituents from the seeds of *Nigella glandulifera* and their hypoglycemic activities†

Qingqing Li,‡[a] Jing Xu,‡[a] Yiyu Chen,[a] Wenli Xie,[a] Gui Mei,[a] Xueni Li,[a] Yu Chen*[b] and Guangzhong Yang *[a]

Received 25th April 2022
Accepted 27th June 2022

DOI: 10.1039/d2ra02628g

rsc.li/rsc-advances

The seeds of *Nigella glandulifera* Freyn et Sint. are traditional Uygur medicine used for the treatment of diabetes. However, the active anti-diabetic constituents in the seeds of *N. glandulifera* remain unclear. In the present study, a new delabellane-type diterpene, 8-denicotinoylnigellamine A1 (**1**), and a new acyclic sesquiterpene, 2,6,10-trimethyl-6,7,12-trihydroxy-dodec-2-ene (**3**), together with eight known compounds including alkaloids (**2** and **7**), triterpenoid saponins (**4**–**6**), and phenolic compounds (**8**–**10**), were isolated from the seeds of *N. glandulifera*. Their structures were determined by extensive spectroscopic analyses and quantum chemical calculations. We evaluated the potential protective effects of the isolated compounds on an insulin resistant HepG2 (IR-HepG2) cell model. The results showed that compounds **2**, **4**–**8**, and **10** could promote the consumption of glucose in IR-HepG2 cells. Those compounds might be responsible for the anti-diabetic effects of the seeds of *N. glandulifera*.

1. Introduction

Type 2 diabetic mellitus (T2DM) is a chronic metabolic disease associated with the abnormal secretion and action of insulin, characterized by hyperglycemia. It is mainly resulting from insulin resistance (IR) or insufficient insulin secretion, also accompanied by abnormal glucose metabolism.[1,2] Improving insulin resistance is an effective method of preventing and treating T2DM. At present, the clinical treatment of T2DM mainly depends on insulin and hypoglycemic drugs by chemical synthesis such as biguanide, sulphonylurea, thiazolidinedione, and meglitinide,[3] which have significant effects but are accompanied by some toxic and side effects.[4–6] It is important to seek safe, effective, and affordable new drugs for the treatment of T2DM.[7] Some natural substances have been considered to be valuable resources for the development of new agents because of their low toxicity and diverse activities.

Nigella glandulifera Freyn et Sint. belongs to the genus of *Nigella* (Ranunculaceae), which is widely distributed in Xinjiang Uygur Autonomous Region of China. The seeds of *N. glandulifera* are widely used in traditional Uygur medicine for the treatment of diabetes, tinnitus, amnesia, amenorrhea, hypokalaemia, and heat stranguria. Previous phytochemical investigations showed that the active constituents of *N. glandulifera* are volatile oil, alkaloids,[8–10] triterpenoid saponins,[11] and flavonoid glycosides.[12] Modern pharmacological results showed that the seeds of *N. glandulifera* had anti-diabetic effects.[13,14] Some alkaloids from the seeds of *N. glandulifera* were reported to have PTP1B inhibitory activity which improved glucose consumption and glycogen synthesis through PI3K/Akt insulin signaling pathway.[15] To explore new anti-diabetic compounds from the seeds of *N. glandulifera*, phytochemical investigations were carried out in the present study. As a result, a new delabellane-type diterpene, 8-denicotinoylnigellamine A1 (**1**), and a new acyclic sesquiterpene, 2,6,10-trimethyl-6,7,12-trihydroxy-dodec-2-ene (**3**), together with eight known compounds were isolated from the seeds of *N. glandulifera* (Fig. 1). Moreover, the hypoglycemic activities of these compounds were investigated using insulin resistance HepG2 cells.

2. Result and discussion

2.1 Structural elucidation of the isolated compounds

Compound **1** was isolated as a white amorphous powder. Its molecular formula was deduced as $C_{34}H_{40}O_6$ from HR-ESI-MS spectrum with a pseudo molecular ion peak at *m*/*z* 567.27148 ($[M + Na]^+$, calcd for $C_{34}H_{40}O_6Na$ 567.27171), corresponding to 15 degrees of unsaturation (DOUs). Careful analysis of the NMR data of **1** (Table 1) displayed the presence of two benzoyl groups. In addition to these NMR data described above, the ^{1}H-NMR spectrum of **1** indicated that **1** contained four methyls [δ_H 1.42 (3H, s); 1.76 (3H, s); 1.80 (3H, s); 1.83 (3H, s)], an oxygenated methylene [δ_H 5.35 (1H, d, J = 10.8 Hz); 4.75 (1H, d, J = 10.8

[a]*School of Pharmaceutical Sciences, South-Central Minzu University, Wuhan 430074, P. R. China. E-mail: yanggz888@126.com; Fax: +86 27 6784 1196; Tel: +86 27 6784 1196*

[b]*College of Chemistry and Material Sciences, South-Central Minzu University, Wuhan 430074, P. R. China. E-mail: chenyuwh888@126.com*

† Electronic supplementary information (ESI) available. See https://doi.org/10.1039/d2ra02628g

‡ These authors contributed equally to this work.

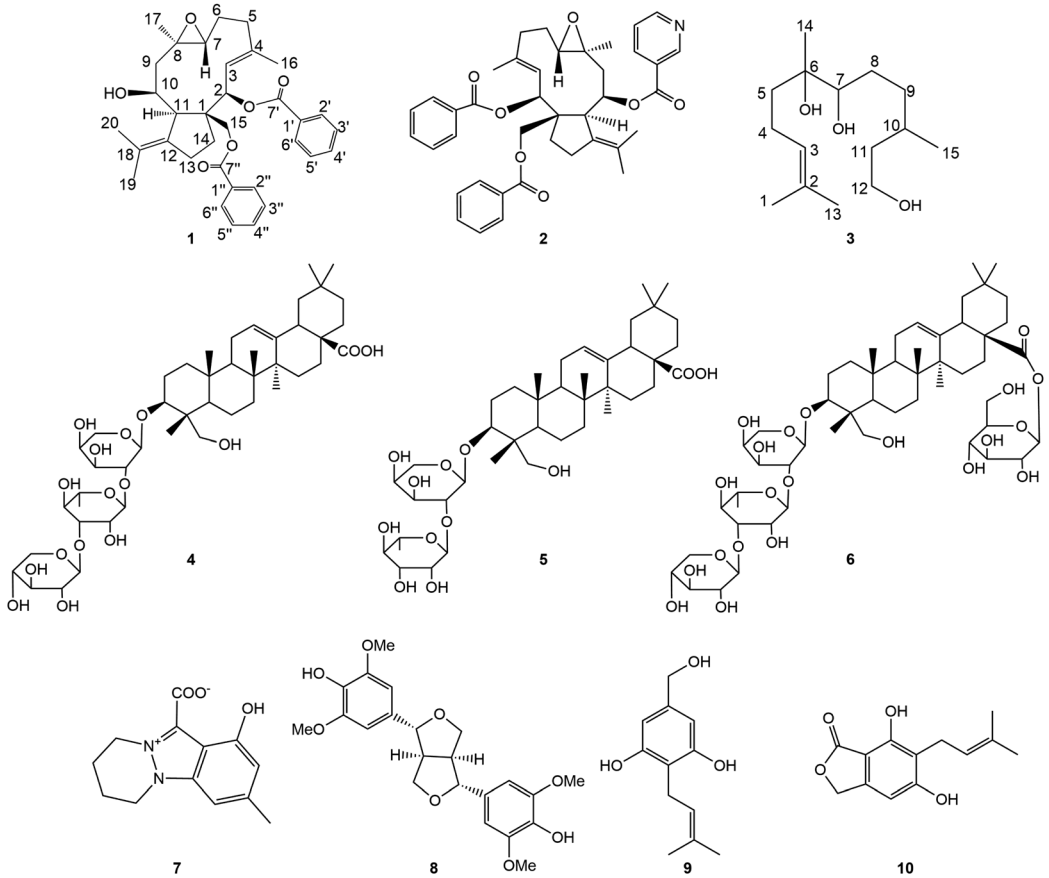

Fig. 1 Structures of the isolated compounds **1–10** from the seeds of *N. glandulifera*.

Hz)], three oxygenated methines [δ_H 5.45 (1H, d, J = 10.2 Hz); 3.10 (1H, d, J = 9.0 Hz); 4.23 (1H, dd, J = 12.6, 4.8 Hz)], one olefinic proton [δ_H 5.75 (1H, d, J = 10.2 Hz)]. The ^{13}C-NMR spectra together with HSQC spectrum indicated the presence of 20 carbon signals, including 5 methines, 4 methyls, 6 methylenes, and 5 quaternary carbons. The above-mentioned

Table 1 ^{1}H and ^{13}C-NMR data of compound **1** (600 MHz, 150 MHz, δ in ppm, J in Hz, CD_3OD)

No	^{1}H-NMR	^{13}C-NMR	No	^{1}H-NMR	^{13}C-NMR
1		58.0	18		126.3
2	5.45 (1H, d, 10.2)	74.7	19	1.76 (3H, s)	22.8
3	5.75 (1H, d, 10.2)	125.3	20	1.83 (3H, s)	22.6
4		141.0	1′		131.5
5	2.47 (1H, m)	38.9	2′	7.72 (1H, dd, 8.4, 1.2)	130.7
	2.35 (1H, m)				
6	1.92 (1H, m)	24.1	3′	7.09 (1H, t, 7.8)	129.5
	1.76 (1H, m)				
7	3.10 (1H, d, 9.0)	67.3	4′	7.44 (1H, m)	134.2
8		60.9	5′	7.09 (1H, t, 7.8)	129.5
9	2.31 (1H, m)	47.6	6′	7.72 (1H, dd, 8.4, 1.2)	130.7
	1.45 (1H, t)				
10	4.23 (1H, dd, 12.6, 4.8)	73.7	7′		168.1
11	2.45 (1H, m)	50.9	1″		132.1
12		140.3	2″	8.09 (1H, dd, 8.4, 1.2)	131.1
13	2.57 (1H, m)	30.0	3″	7.44 (1H, m)	129.9
	2.36 (1H, m)				
14	2.25 (2H, m)	32.6	4″	7.63 (1H, td, 7.2, 1.2)	134.5
15	5.35 (1H, d, 10.8)	68.8	5″	7.44 (1H, m)	129.9
	4.75 (1H, d, 10.8)				
16	1.80 (3H, s)	17.0	6″	8.09 (1H, dd, 8.4, 1.2)	131.1
17	1.42 (3H, s)	19.1	7″		168.4

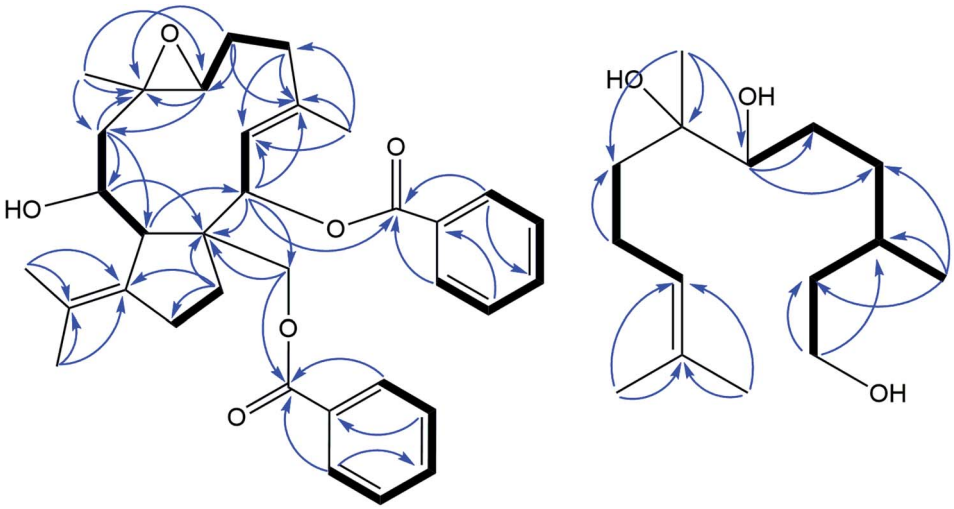

Fig. 2 $^{1}H-^{1}H$ COSY and HMBC correlations for compounds **1** and **3**.

evidence indicated that **1** belonged to a dolabellane-type diterpene with two benzoyl groups. Compared with NMR data of nigellamine A1, **1** had one less nicotinoyl signal, suggesting that **1** was denicotinoylated of nigellamine A1.[16] The chemical shifts of H-10 being shifted upfield from δ_H 5.70 in nigellamine A1 to δ_H 4.23 in **1** confirmed the above inference. HMBC correlations (Fig. 2) from H-2 to C-7′, and H_2-15 to C-7″ confirmed two benzyloxy groups were connected to C-2 and C-15 respectively. Consequently, the planar structure of **1** was determined. Detailed analysis of ROESY spectrum (Fig. 3) suggested that the relative configuration of **1** was the same as that of nigellamine A1. ROESY correlations of H-2 with H-11; H-10 with CH_3-17 and H-11; H-7 with H-3 and H_2-15 showed that H-2, H-10, H-11, and CH_3-17 were cofacial and arbitrarily determined as α-configuration. Instead, H-7 and H_2-15 were on the other side and arbitrarily determined as β-configuration. Therefore, the relative configuration of **1** was accurately determined as shown in Fig. 1. Based on the modified allylic benzoate rule and ECD calculations, the absolute configuration of **1** was resolved.[16,17] The CD spectrum of **1** displayed a positive cotton effect (CE) at 238 nm, and the optical rotation value of **1** showed dextrorotation, which was contrary to nigellamine A1 (**2**). These findings suggested that the absolute configuration of **1** was the same as the enantiomer of nigellamine A1. Furthermore, the ECD calculations for (1*S*, 2*S*, 7*S*, 8*S*, 10*R*, 11*S*)-**1a** and its enantiomer (1*R*, 2*R*, 7*R*, 8*R*, 10*S*, 11*R*)-**1a**′ were carried out by the TDDFT/ECD method at the B3LYP/6-31+G(d) level. The results showed that the calculated ECD data of (1*R*, 2*R*, 7*R*, 8*R*, 10*S*, 11*R*)-**1a**′ was consistent with the experimental ECD data. Thus, the absolute configuration of **1** was determined as depicted in Fig. 4.

Compound (**3**) was purified as a slight yellow oil and assigned the molecular formula as $C_{15}H_{30}O_3$ by HR-ESI-MS spectrum with a pseudo molecular ion peak at *m*/*z* 281.20871 ($[M + Na]^+$, calcd for $C_{15}H_{30}O_3Na$, 281.20872), corresponding to one degree of unsaturation (DOUs). In the UV spectrum, the maximum absorption observed at 205 nm showed that **3** had no obvious conjugate system. The ^{1}H-NMR spectrum of **3** (Table 2) exhibited one olefin proton [δ_H 5.32 (td, J = 7.2, 1.2 Hz)], three tertiary methyl groups [δ_H 1.61 (s), 1.67 (s), 1.49 (s)], one

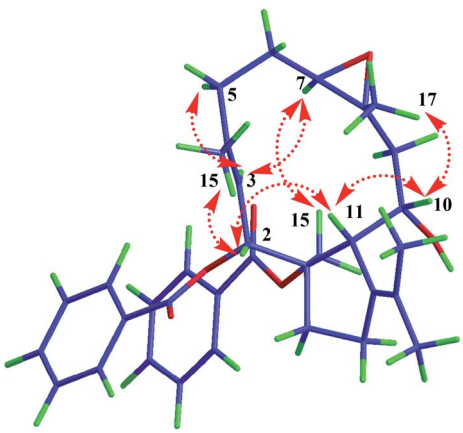

Fig. 3 Key ROESY (HH) correlations of compound **1**.

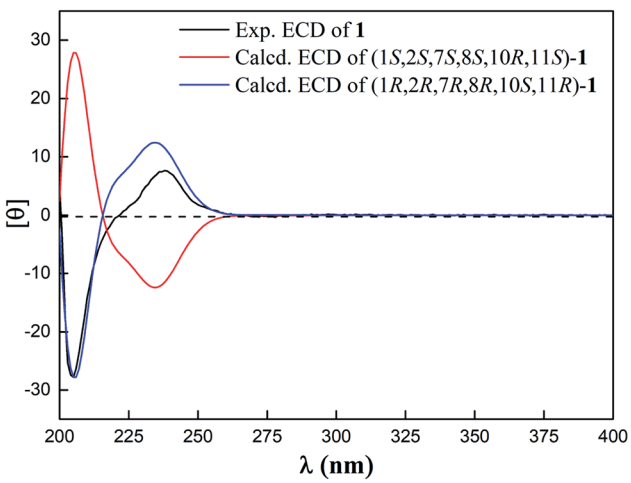

Fig. 4 Calculated ECD spectrum of and experimental ECD curves of **1**.

Table 2 ^{1}H and ^{13}C-NMR data of compound **3** (600 MHz, 150 MHz, δ in ppm, J in Hz, C_5D_5N)

No	^{1}H-NMR	^{13}C-NMR	No	^{1}H-NMR	^{13}C-NMR
1	1.61 (3H, s)	18.0	8	2.01 (1H, m) 1.81 (1H, m)	29.8
2		131.0	9	1.87 (1H, m) 1.70 (1H, m)	35.7
3	5.32 (1H, td, 7.2, 1.2)	126.6	10	1.93 (1H, m)	30.5
4	2.59 (1H, m) 2.42 (1H, m)	23.1	11	1.90 (1H, m) 1.62 (1H, m)	41.6
5	2.10 (1H, td, 13.2, 4.8) 1.83 (1H, m)	39.1	12	3.96 (2H, m)	60.6
6		74.6	13	1.67 (3H, s)	26.2
7	3.82 (1H, d, 10.8)	78.8	14	1.49 (3H, s)	23.5
			15	0.99 (3H, d, 6.6)	20.3

secondary methyl [δ_H 0.99 (d, J = 6.6 Hz)], an oxygenated methylene [δ_H 3.96 (2H, m)], one oxygenated methines [δ_H 3.82 (1H, d, J = 10.8 Hz)]. Detail analysis of ^{13}C-NMR, DEPT combined with HSQC spectrum displayed 15 carbon signals assignable to four methyls, three methines (including one sp^2 carbon at δ_C 126.6 and one oxygenated carbon at δ_C 78.8), six methylenes (including one oxygenated carbon at δ_C 60.6), one oxygenated tertiary carbon at δ_C 74.6, one sp^2 quaternary carbon at δ_C 131.0. The above-mentioned data indicated that **3** belonged to an acyclic sesquiterpene with three hydroxy groups and one double bond. Further analysis of the ^{1}H–^{1}H COSY, HSQC, and HMBC spectra led to the elucidation of two structural fragments as a 4-methyl-3-pentenyl and 4-methyl-1,6-hexanediol group. The HMBC correlations from H_3-14 to C-5, C-6, and C-7 showed that CH_3-14 and 4-methyl-3-pentenyl linked to 4-methyl-1,6-hexanediol group through one oxygen tertiary carbon C-6 [δ_C 74.6 (s)]. Therefore, the structure of compound **3** was determined as shown.

The remaining eight known compounds were identified as nigellamine A1 (**2**),[16] 3-*O*-[β-D-xylopyranosyl-(1 → 3)-α-L-rhamnopyranosyl-(1 → 2)-α-L-arabinpyranosyl]-hederagenin (**4**),[18] α-hederin (**5**),[18] decaisoside E (**6**),[19] nigellicine (**7**),[20] yangambin (**8**),[21] nigephenol A (**9**),[22] 5,7-dihydroxy-6-(3-methybut-2-enyl) isobenzofuran-(13*H*)-one (**10**)[23] by comparison spectroscopic data with the literature data.

2.2 Glucose consumption of IR-HepG2 cells

The seeds of *N. glandulifera* exhibit multiple biological activities, such as being anti-inflammatory, anti-diabetic, anti-oxidative and hepatoprotective.[24–27] *N. sativa*, another commonly used medical plant belongs to the same genus, exerts anti-diabetic and immune-modulatory effects.[28,29] Based on the distinct hypoglycemic activities, anti-diabetic effects of the constituents from these plants were further analyzed. The alkaloids, such as nigelladines A-C, exert an anti-diabetic effect by activating PI3K/Akt insulin signaling pathway and inhibiting PTP1B.[13] In the present study, phytochemical investigation of the seeds of *N. glandulifera* led to the isolation of three structural types of natural products, including terpenes (**1–6**), alkaloids (**7**), and phenolic compounds (**9** and **10**). The anti-diabetic effects of these compounds were still unknown. The major contributor to the pathogenesis of T2DM is IR, which refers to the decreased responsiveness of peripheral blood cells (liver, muscle, and adipose tissue) to glucose metabolism, resulting in an abnormal homeostatic response to blood glucose.[30] For the establishment of IR model, human hepatoblastoma HepG2 cells were used as reported.[31] Moreover, metformin was chosen as the positive control because it could promote hepatic glucose consumption in IR HepG2 cells.[32–34] The hypoglycemic activity of these isolated compounds was determined using the IR-

Table 3 Effect of compounds **1–10** on the cell viability in HepG2 cells

	Cell viability						
Compound	0 μM	10 μM	20 μM	30 μM	40 μM	50 μM	IC_{50} (μM)
1	100.00%	97.27 ± 3.45%	93.91± 3.05%	90.71 ± 2.77%	76.58 ± 2.77%	68.00 ± 2.91%	68.07
2	100.00%	97.19 ± 1.04%	93.08 ± 1.43%	91.01 ± 0.97%	87.66 ± 0.84%	87.70 ± 1.57%	308.3
3	100.00%	94.76 ± 1.94%	83.50 ± 3.68%	60.27 ± 3.33%	36.31 ± 1.62%	33.36 ± 1.90%	33.95
4	100.00%	96.11 ± 2.98%	93.05 ± 3.98%	85.90 ± 0.77%	82.95 ± 0.51%	76.91 ± 2.78%	120.2
5	100.00%	98.57 ± 0.57%	93.39 ± 1.23%	89.38 ± 1.16%	76.11 ± 1.73%	73.33 ± 2.58%	98.49
6	100.00%	96.33 ± 1.34%	92.23 ± 0.55%	87.40 ± 1.81%	84.46 ± 3.47%	69.35 ± 1.71%	185.4
7	100.00%	99.30 ± 1.45%	92.32 ± 1.02%	78.38 ± 2.34%	73.81 ± 3.72%	68.36 ± 2.16%	72.56
8	100.00%	94.52 ± 5.42%	92.59 ± 1.39%	80.22 ± 3.79%	76.22 ± 1.66%	68.57 ± 2.12%	78.61
9	100.00%	96.59 ± 2.83%	99.78 ± 2.92%	89.44 ± 2.28%	78.22 ± 3.65%	62.37 ± 4.10%	56.08
10	100.00%	94.50 ± 2.24%	93.27 ± 1.28%	91.06 ± 0.79%	87.28 ± 2.54%	75.33 ± 1.89%	96.76

Table 4 Glucose consumption of compounds **1**-**10** in IR-HepG2 cells[a] (mM)

Compound	NG	MG	Met	Concentration				
				2.5 μM	5.0 μM	10.0 μM	12.5 μM	15 μM
1	5.90 ± 0.56	3.47 ± 0.77	8.49 ± 0.79	3.92 ± 0.61	4.59 ± 0.45	4.71 ± 0.17	5.60 ± 0.47	5.56 ± 0.69
2	6.08 ± 0.30	3.74 ± 0.62	9.90 ± 0.42	4.77 ± 0.79	7.01 ± 0.72	6.98 ± 0.72	7.90 ± 0.52	8.56 ± 0.58
3	5.82 ± 0.81	1.33 ± 0.43	9.42 ± 0.41	2.06 ± 1.27	2.43 ± 0.67	2.66 ± 0.56	2.86 ± 0.71	2.44 ± 0.60
4	5.26 ± 0.53	2.09 ± 0.66	8.82 ± 0.53	5.75 ± 0.39	6.95 ± 0.71	7.38 ± 0.62	8.32 ± 0.61	8.59 ± 0.73
5	5.49 ± 0.40	2.90 ± 0.48	9.48 ± 0.64	6.31 ± 0.96	6.95 ± 0.22	7.75 ± 0.84	8.97 ± 0.37	9.99 ± 0.95
6	6.25 ± 0.40	2.91 ± 0.84	9.52 ± 0.26	5.67 ± 0.76	5.93 ± 0.94	8.59 ± 1.46	9.73 ± 0.39	11.97 ± 0.72
7	5.53 ± 0.29	2.45 ± 0.55	9.20 ± 0.59	6.75 ± 0.51	8.01 ± 0.56	8.47 ± 0.46	9.01 ± 0.50	9.48 ± 0.93
8	5.81 ± 0.17	2.45 ± 0.86	9.78 ± 0.83	6.47 ± 0.17	7.97 ± 0.57	8.25 ± 0.34	8.97 ± 0.47	9.76 ± 0.48
9	5.67 ± 0.59	3.50 ± 0.40	9.87 ± 0.79	4.64 ± 0.57	4.24 ± 0.92	4.77 ± 0.47	4.79 ± 0.65	4.51 ± 0.76
10	5.98 ± 0.20	2.97 ± 0.93	9.49 ± 0.51	8.96 ± 0.90	9.15 ± 0.90	9.15 ± 0.38	10.57 ± 0.84	11.01 ± 0.86

[a] NG: normal group; MG: model group; Met: metformin.

HepG2 cell model. Firstly, cell viabilities of all isolated compounds were evaluated by CCK-8 method. As shown in Table 3, all isolated compounds showed no significant effects on the viability of HepG2 cells at concentrations below 20 μM. Therefore, five concentrations of 2.5, 5, 10, 12.5, and 15 μM (cell viability > 90%) were used for further analysis. As shown in Table 4, compared to the normal group, the glucose consumption of the model group was significantly decreased, which demonstrated IR-HepG2 cell model was successfully built up. At a concentration of 5 μM of compounds **2**, **4–8**, **10,** the glucose consumption increased to 5.93–9.15 mM which had no significant difference from the normal group. Among them, the glucose consumption of compound **10** at 12.5 and 15 μM were 10.57 ± 0.84 and 11.01 ± 0.86 mM, respectively, both of which were higher than the positive control of metformin (9.49 ± 0.51 mM). Triterpenoid saponins (**4–6**) significantly increased glucose consumption in IR-HepG2 cell model at 15 μM. These findings showed that these compounds could improve the IR of HepG2 cells and may have anti-diabetic effects.

3. Experimental section

3.1 General experimental procedures

Optical rotations were measured in MeOH on an Autopol IV polarimeter (Rudolph Research Analytical, Hackettstown, NJ, USA). UV spectra was obtained on a UH5300 UV-VIS Double Beam spectrophotometer (Hitachi Co., Tokyo, Japan). ECD spectra was recorded on a Chirascan Plus spectrometer (Applied Photophysics Ltd, London, England). 1D and 2D NMR spectra were recorded on a Bruker AVANCE IIITM 500 MHz or 600 MHz spectrometers (Bruker, Ettlingen, Germany) using tetramethylsilane (TMS) as an internal reference standard. Chemical shifts (δ) have been expressed in ppm and the coupling constants (J) have been given in Hz. High-resolution electrospray mass spectroscopy was performed on a Thermo Scientific Q Exactive Orbitrap LC-MS/MS System (HR-ESI-MS) (Thermo Scientific, Waltham, MA, USA). High-performance liquid chromatography (HPLC) was conducted on an Ultimate 3000 HPLC system (Dionex Co., Sunnyvale, CA, USA) equipped with an Ultimate 3000 pump and Ultimate 3000 Variable Wavelength detector, as well as a semi-preparative YMC-Pack ODS-A column (250 × 10 mm, 5 μm) and a preparative YMC-Pack ODS-A column (250 × 20 mm, 5 μm) from YMC Co., Ltd (Kyoto, Japan), column chromatography (CC) was conducted on silica gel (200–300 mesh and 300–400 mesh, Qingdao Haiyang Chemical Industry Co., Ltd., Qingdao, China). Chromatographic grade acetonitrile was purchased from Chang Tech Enterprise Co., Ltd (Taiwan, China). Dulbecco's Modified Eagle Medium (DMEM) and 0.25% pancreatin were obtained from Wuhan Procell Life Science Technology Co., Ltd. (Wuhan, China). The glucose kit was obtained from Shanghai Rongsheng Biotech Co., Ltd. (Shanghai, China). Metformin hydrochloride tablets were obtained from Sino-American Shanghai Squibb Pharmaceuticals Ltd. (Shanghai, China). Cell counting kit-8 (CCK8) was obtained from ABclonal Technology Co., Ltd. (Wuhan, China). Glucose solution and palmitate acid (PA) were obtained from Sigma-Aldrich Co., Ltd. (St. Louis, MO, USA). Fetal bovine serum (FBS) was obtained from Zhejiang Tianhang Biotechnology Co., Ltd. (Hangzhou, China).

3.2 Plant materials

Dried seeds of *N. glandulifera* were acquired in October 2018 from Xinjiang Uygur Autonomous Region, P. R. China, and identified by Prof. Xinqiao Liu, School of Pharmaceutical Sciences, South-Central Minzu University. The voucher specimens were deposited in the herbarium of School of Pharmaceutical Sciences, South-Central Minzu University.

3.3 Extraction and isolation

Dried seeds of *N. glandulifera* (9.8 kg) were defatted with petroleum ether three times, and then extracted with 50% EtOH three times (12 h each time) at room temperature. The combined EtOH extracts were evaporated under vacuum to yield crude extract, and then suspended in the distilled water, and extracted successively with ethyl acetate (EtOAc), n-butanol to yield EtOAc extract (120 g), and n-butanol extract (140 g). The EtOAc extract was isolated by silica gel column chromatography, using petroleum ether-CH_2Cl_2–MeOH gradient as **eluent** to yield 7 fractions (Fr. A.1 ∼ Fr. A.7). Fr. A.3 (2.8 g) was

repeatedly fractionated by normal and reversed phase silica gel chromatographic column and further purified by semi-preparative HPLC to obtain compound **1** (1.0 mg, MeOH-0.1% formic acid, 78 : 22, t_R = 40.2 min), **2** (1.0 mg, MeOH-0.1% formic acid, 85 : 15, t_R = 28.0 min), **8** (2.0 mg, MeCN–H_2O, 78 : 22, t_R = 38.5 min). Fr. A.5 (2.0 g) was subjected to repeated ODS CC with MeOH–H_2O (30 : 70 to 90 : 10) and semi-preparative HPLC to afford compound **3** (2 mg, MeCN–H_2O, 37 : 63, t_R = 19.1 min), **7** (2 mg, MeCN-0.1% formic acid = 23 : 77, t_R = 25.8 min) and **9** (2 mg, MeCN–H_2O, 25 : 75, t_R = 30.1 min). Fr. A.6 (2.8 g) was purified by ODS CC, using MeOH–H_2O gradient (30 : 70 to 90 : 10) as eluent, to yield 7 fractions (Fr. A.6.1–Fr. A.6.7). Fr. A.6.2 was separated by semi-preparative HPLC to afford compound **10** (2 mg, MeCN–H_2O, 42 : 58, t_R = 22.3 min). The n-butanol extract was applied to D101 macroporous resin using H_2O–EtOH as eluent to give 12 fractions. Fr. B.11 and Fr. B.12 were purified by repeated semi-preparative HPLC to afford compound **4** (50.0 mg, MeOH-0.1% formic acid, 77 : 23, t_R = 26.1 min), **5** (10.0 mg, MeOH-0.1% formic acid, 77 : 23, t_R = 28.2 min), **6** (1.0 mg, MeOH-0.1% formic acid, 70 : 30, t_R = 20.0 min).

8-denicotinoy.lnigellamine A_1 (**1**): white amorphous powder; $[\alpha]_D^{24}$ = +25.0° (*c* 0.19, MeOH); UV (MeOH) λ_{max} (log ε): 230 (4.46), 270 (3.46) nm; ECD (3.47 × 10^{-3} M, MeOH) $\lambda(\theta)$: 204 (−27.40), 238 (+7.62) nm; ^{1}H-NMR (600 MHz, $CDCl_3$) and ^{13}C-NMR (150 MHz, $CDCl_3$): see Table 1; HR-ESI-MS *m*/*z* 567.27148 [M + Na]+(calcd for $C_{34}H_{40}O_6Na$, 567.27171).

2,6,10-trimethyl-6,7,12-trihydroxy-dodec-2-ene (**3**): light yellow oil; $[\alpha]_D^{24}$ = +11.3° (*c* 0.20, MeOH); UV (MeOH) λ_{max} (log ε): 205 (3.22) nm; ^{1}H-NMR (600 MHz, C_5D_5N) and ^{13}C-NMR (150 MHz, C_5D_5N) see Table 2; HR-ESI-MS *m*/*z* 281.20871 [M + Na]+(calcd for $C_{15}H_{30}O_3Na$, 281.20872).

3.4 ECD calculation

The absolute configuration of **1** was determined by quantum chemical TDDFT calculation of its theoretical ECD spectrum according to a previously reported method.[35]

3.5 Cell viability

HepG2 cells (1.0 × 10^5 cells/well) were grown in a 96-well plate at 37 °C in a DMEM medium containing 15% fetal bovine serum. After treatment with different concentrations of compounds **1–10** (10, 20, 30, 40, and 50 μM) for 24 h, the supernatant was removed. 100 μL DMEM and 10% CCK-8 were added to each well, and incubated at 37 °C for 30 min. The absorbance was measured at 450 nm with a microplate analyzer to calculate the cell viability.

3.6 Glucose consumption in IR-HepG2 cells

The IR-HepG2 cell model was induced by palmitic acid (PA) as previously reported.[36,37] Briefly, after 12 h serum-free starvation, HepG2 cells were cultured in high glucose (30 mM) DMEM plus PA (0.25 mM) as the model group, and high glucose DMEM plus PA in the presence of compounds **1–10** with different concentrations (2.5, 5.0, 10, 12.5 and 15 μM) for 24 h. The glucose concentration in the medium was determined using a glucose assay kit (Nanjing Jiancheng Bioengineering Institute) according to the instruction. The amount of glucose consumption was calculated by the initial glucose level minus the glucose level remaining in the medium. Metformin hydrochloride (2 mM) was used as the positive control.

4. Conclusion

In summary, phytochemical studies on the seeds of *N. glandulifera* resulted in the separation of two previously undescribed compounds (**1** and **3**) together with eight known compounds (**2**, **4–10**), including two dolabellane diterpenes (**1 and 2**), one acyclic sesquiterpene (**3**), triterpene saponins (**4–6**), one alkaloid (**7**), and three phenolic compounds (**8–10**). Moreover, the hypoglycemic activity of the isolated compounds was determined by the IR-HepG2 cell model. The results showed compounds **2**, **4–8**, **10** could promote the glucose consumption of IR-HepG2 cell. These findings illuminate the active compounds of the seeds of *N. glandulifera* in the treatment of T2DM and may offer new strategies for alleviating the hepatic IR of T2DM.

Author contributions

YC and GY: conceptualization, writing, reviewing and editing; QL: purification and isolation of compounds, writing-original draft; XJ: hypoglycemic activity assay; WX: ECD calculations; YYC, GM and XL: formal analysis, data curation.

Conflicts of interest

The authors declare that there is no conflict of interest.

Acknowledgements

This work was supported by the Research and Development Program of Hubei Province (2021ACB003), and the Major Scientific, Technological Project of Hubei Province (2020ACA007) and the Special Fund for Basic Scientific Research of Central Colleges, South-Central University for Nationalities (CZY22002).

References

1 D. D. Huang, G. J. Shi, Y. P. Jiang, C. Chao and C. L. Zhu, *Biomed. Pharmacother.*, 2020, **125**, 109767.
2 N. Ning, E. Kim, B. Li, H. B. Pan, T. T. Tong, C. S. Yang and Y. Y. Tu, *J. Agric. Food Chem.*, 2019, **67**, 5361–5373.
3 G. E. C. Sun, B. J. Wells, K. Yip, R. Zimmerman, D. Raghavan, M. W. Kattan and S. R. Kashyap, *Diabetes, Obes. Metab.*, 2014, **16**, 276–283.
4 S. Okayasu, K. Kitaichi, A. Hori, T. Suwa, Y. Horikawa, M. Yamamoto, J. Takeda and Y. Itoh, *Biol. Pharm. Bull.*, 2012, **35**, 933–937.
5 D. Desilets, A. Shorr, K. Moran and K. Holtzmuller, *Am. J. Gastroenterol.*, 2001, **96**, 2257–2258.
6 F. W. Germino, *Clin. Ther.*, 2011, **33**, 1868–1882.

7 Z. Z. Gao, Q. W. Li, X. M. Wu, X. M. Zhao, L. H. Zhao and X. L. Tong, *J. Immunol.*, 2017, **2017**, 1813086.
8 J. Tian, C. Han, W. Guo, Y. Yin, X. Wang, H. Sun, H. Yao, Y. Yang, C. Wang, C. Liu, M. Yang and L. Kong, *Org. Lett.*, 2017, **19**, 6348–6351.
9 Y. Liu, L. Sun, Q. Liu, S. Lu and B. Chen, *Biochem. Syst. Ecol.*, 2013, **49**, 43–46.
10 W. Guo, X. Li, S. Huang, M. Yang and L. Kong, *J. Asian Nat. Prod. Res.*, 2017, **19**, 9–14.
11 X. Xin, H. A. Aisa, H. Q. Xue and H. Q. Wang, *Chem. Nat. Compd.*, 2008, **44**, 134–136.
12 B. Boubertakh, X. G. Liu, X. L. Cheng and P. Li, *J. Chem.*, 2013, **2013**, 820183.
13 Y. L. Zheng, Q. Zhang and X. J. Hu, *Med. Chem. Res.*, 2020, **29**, 1168–1186.
14 Y. Niu, L. Zhou, L. Meng, S. Chen, C. Ma, Z. Liu and W. Kang, *J. Evidence-Based Complementary Altern. Med.*, 2020, 6756835.
15 Y. Ma, J. Li, F. Tong, X. L. Xin and H. A. Aisa, *Ind. Crops Prod.*, 2020, **153**, 112592.
16 T. Morikawa, F. M. Xu, Y. Kashima, H. Matssuda, K. Ninomiya and M. Yoshikawa, *Org. Lett.*, 2004, **6**, 869–872.
17 T. Morikawa, F. M. Xu, K. Ninomiya, H. Matssuda and M. Yoshikawa, *Chem. Pharm. Bull.*, 2004, **52**, 494–497.
18 Y. M. Liu, J. S. Yang and Q. H. Liu, *China J. Chin. Mater. Med.*, 2005, **30**, 980–983.
19 J. Kong, X. H. Yang, R. H. Lu, Y. P. Wang and H. Q. Wang, *Indian J. Chem.*, 1999, **37b**, 882–884.
20 A. Rahman, S. Malik, C. H. He and J. Clardy, *Tetrahedron Lett.*, 1985, **26**, 2759–2762.
21 N. M. Lima, L. M. Cursino-Hron, A. M. Lima, J. B. V. Souza, A. C. Oliveira, J. V. N. Marinhoa and C. V. Nunez, *Rev. Bras. Farmacogn.*, 2018, **28**, 697–702.
22 L. Sun, Y. M. Liu, B. Q. Chen and Q. H. Liu, *Bioorg. Med. Chem. Lett.*, 2015, **25**, 3864–3866.
23 G. H. Li, L. Li, M. Duan and K. Q. Zhang, *Chem. Biodiversity*, 2006, **3**, 210–216.
24 D. Tang, Q. B. Chen, X. L. Xin and H. A. Aisa, *Biomed. Pharmacother.*, 2017, **87**, 145–152.
25 J. B. Gao, X. J. Zhang, R. H. Zhang, L. L. Zhu, D. B. Pu, X. L. Li, H. L. Li, M. Xu and W. L. Xiao, *Planta Med.*, 2018, **84**, 1013–1021.
26 D. Maimaitiyiming, M. Kamilijiang, X. Xiaerfuding, S. W. Hui, M. Abudureyimu, Hajinisha and A. Aikemu, *Pak. J. Pharm. Sci.*, 2017, **30**, 1567–1571.
27 H. Jiang, F. Xu, L. Zeng, C. Li, Y. Chen, L. Wang, Z. Li and R. Liu, *J. Ethnopharmacol.*, 2022, **283**, 114714.
28 J. Dong, Q. Liang, Y. Niu, S. Jiang, L. Zhou, J. Wang, C. Ma and W. Kang, *Int. J. Biol. Macromol.*, 2020, **159**, 725–738.
29 Y. Niu, B. Wang, L. Zhou, C. Ma, G. I. N. Waterhouse, Z. Liu, A. F. Ahmed, D. Sun-Waterhouse and W. Kang, *Front. Nutr.*, 2021, **8**, 722813.
30 J. C. Chen, L. Li, X. Zhang, L. T. Wan, Q. S. Zheng, D. Xu, Y. T. Li, Y. Liang, M. S. Chen, B. Li and A. Y. Chen, *J. Funct. Foods*, 2021, **82**, 104478.
31 Z. C. Yang, W. Huang, J. S. Zhang, M. Xie and X. W. Wang, *Eur. J. Pharmacol.*, 2019, **854**, 187–193.
32 Q. Wei, Y. Zhan, B. Chen, B. Xie, T. Fang, S. Ravishankar and Y. Jiang, *Food Sci. Nutr.*, 2020, **8**, 332–339.
33 K. A. Akinyede, H. A. Oyewusi, G. D. Hughes, O. E. Ekpo and O. O. Oguntibeju, *Molecules*, 2021, **27**, e155.
34 A. P. A. Nwakiban, S. Cicolari, S. Piazza, F. Gelmini, E. Sangiovanni, G. Martinelli, L. Bossi, E. Carpentier-Maguire, A. D. Tchamgoue, G. Agbor, J. R. Kuiate, G. Beretta, M. Dell'Agli and P. Magni, *Metabolites*, 2020, **10**, e182.
35 X. Tan, X. Y. Han, H. D. Teng, Q. Q. Li, Y. Chen, X. X. Lei and G. Z. Yang, *J. Nat. Prod.*, 2021, **8**, 972–978.
36 J. R. Nie, Y. N. Chang, Y. Li, Y. Zhou, J. Qin, Z. Sun and H. B. Li, *J. Agric. Food Chem.*, 2017, **65**, 9041–9053.
37 Y. Zhang, S. G. Chen, C. Y. Wei, J. C. Chen and X. Q. Ye, *J. Funct. Foods*, 2017, **29**, 217–225.